Article

Not peer-reviewed version

Investigation on the Performance of Battery Thermal Management Based Direct Refrigerant Cooling: Simulation, Validation of Results and Parametric Studies

Suparat Jamsawang , Saharat Chanthanumataporn * , Kittiwoot Sutthivirode , Tongchana Thongtip *

Posted Date: 7 December 2023

doi: 10.20944/preprints202312.0502.v1

Keywords: BTMS; Refrigerant Cooling; Evaporation heat transfer; EVs

Article

Investigation on the Performance of Battery Thermal Management Based Direct Refrigerant Cooling: Simulation, Validation of Results and Parametric Studies

Suparat Jamsawang [1], Saharat Chanthanumataporn [1,*], Kittiwoot Sutthivirode [2] and Tongchana Thongtip [2,*]

[1] Department of Mechanical and Automotive Engineering, The Sirindhorn International Thai-German Graduate School of Engineering (TGGS), King Mongkut's University of Technology North Bangkok, Bangkok, Thailand

[2] Advanced Refrigeration and Air Conditioning Laboratory (ARAC), Department of Teacher Training in Mechanical Engineering, King Mongkut's University of Technology North Bangkok, 1518 Phacharat 1 Rd., Bang Sue, Bangkok 10800, Thailand

* Correspondence: saharat.c@tggs.kmutnb.ac.th (S.T.); tongchana.t@kmutnb.ac.th (T.T.)

Abstract: This paper proposes a simulation technique for investigating the battery thermal management system based direct refrigerant cooling (BTMS-DRC). It employs finite element method for a combined-conduction-convection heat transfer to predict the module temperature and to prove the temperature uniformity. The refrigerant side cooling is based on the two-phase flow evaporation which is represented by the convection heat transfer (flow evaporation) under a certain refrigerant saturation temperature. The battery heat generation is modeled as the constant heat flux. The main module is modeled as the conduction heat transfer. The real BTMS-DRC is constructed for experimentation with the test bench which is based on the dual-evaporators vapour compression refrigeration system. The simulated result is validated with the experimental results to ensure the correction of the modelling. The simulation also investigates the impact of the heat generation, convection heat transfer coefficient, refrigerant saturation temperature, and thermal conductivity on the module temperature and temperature uniformity. It is found that the simulated results agree well with the experimental results. The errors are around 2.9 - 7.2% throughout the specified working conditions. Overall, the proposed technique can be used as a design tool for further developing the BTMS-DRC.

Keywords: BTMS; refrigerant cooling; evaporation heat transfer; EVs

1. Introduction

Due to batteries serving as the power source for electric vehicles (EVs), heat generation in both charging and discharging states is always produced. This heat is accumulated within the module battery pack which has a negative impact on the battery. The accumulated heat not only affects the battery's operational efficiency; it also reduces its lifespan. If the accumulated heat within the module battery is too high, thermal runaway can occur which leads to explosions and potential fires [1–5].

The battery thermal management (BTMS) plays a crucial role in the efficient operation of the battery pack which yields a longer lifespan. It also serves as a protection system against explosions and battery fires resulting from heat accumulation. This has encouraged many researchers to develop the BTMS via different cooling methods as proposed by Olabi et al. [6] and Luo et al. [7]. Their aim was to maintain the BTMS temperature at around 25 – 35 °C which is recognized as the suitable operating temperature of the Li-ion battery [8–10].

The existing works proposed by Akinlabi et al. [11], Wang et al. [12], Chen et al. [13] concentrated on the air-cooled technique for the BTMS via force convection. This method depends on the ambient

 doi:10.20944/preprints202312.0502.v1

air temperature and air velocity. Hence, at the high ambient temperature, it was unable to work efficiently because the module temperature was too high. Therefore, some researchers employed the water-cooled method to absorb heat from the module battery pack as proposed by Jouhara et al. [14], Kalaf et al. [15] Siruvuri and Budarapu et al. [16], and Siruvuri et al. [17]. They used a liquid pump, a storage tank, and a fin-tube heat exchanger to rejecting heat to the surroundings. The water is pumped to cool down the BTMS module, and heat from the battery is then rejected to surroundings by a fin-tube air-cooled heat exchanger. This method still has limitations due to the ambient temperatures and may not be suitable for use in a quite high ambient temperature. This problem is solved by some researchers by adding a small chiller machine to produce chilled water at the desired temperatures, which allows the BTMS temperature to be controlled precisely. The use of a chiller system allows precise control of the cooling plate temperature, enhancing the accuracy and efficiency of heat transfer. This led to better control of heat dissipation rates. However, using the chilled water for cooling sometimes produces a non-uniform temperature in the BTMS module at a higher heat rate due to the sensible heat transfer. This results in a larger difference in temperature between battery cells (should not exceed 5 °C [18]) which affects the power capacity and lifespan of the battery. Additionally, it is noticeable that using a chiller for the BTMS requires a refrigeration system and water storage for system operation. This results in a more complex system operation than that in other cooling techniques. Additionally, the use of electricity for this cooling system is an important factor for applying it for real use in EVs.

Alternatively, some researchers have proposed a direct refrigerant cooling system for BTMS, as proposed by Hong et al. [19], Wang et al. [20], Cen et al. [21], and Gillet et al. [22]. In their studies, the BTMS is powered by a vapour compression refrigeration system, and the refrigerant is applied to the cooling plate for heat absorption. This cooling plate is designed to allow the liquid refrigerant from the refrigeration system to be directly expanded through the cooling plate. Hence, it then works as an evaporator which can absorb the accumulated heat from the module battery pack. The experimental works by Ren et al. [23] and Chen et al. [24] also indicated that the thermal management by the direct refrigerant cooling is efficient and requires less electrical energy compared to water-based cooling systems. Additionally, it was found that this system has the potential to be integrated into the vehicle's air conditioning system (working as multi cooling purposes). This is made possible by the dual-evaporators vapour compression refrigeration system. However, there are some drawbacks when using the DRC. First, it is quite difficult to control the temperature of the cooling plate at the optimal range. This will produce a too low temperature for the BTMS which has a negative impact on the battery performance. Second, there is still too large a difference in temperature between battery cells (exceeds 5 °C) due to the problem of heat absorption. This is a challenge in this research field. Third, the precise control of the refrigerant flow rate through the BTMS to achieve the proper working BTMS temperature is a problem to be further developed which is a research challenge.

According to the refrigerant flowing through the BTMS (which is a small channel flow equipment), if the refrigerant flow rate is high enough, the flow evaporation of the two-phase fluid will take place within the refrigerant side cooling (small channel or small tubes are mostly used) [26–29]. Hence, the heat transfer from batteries to the refrigerant occurs under the saturated temperatures of the refrigerant as flowing through the BTMS (working as an evaporator). This process comes with the latent heat transfer due to the two-phase refrigerant being evaporated inside. Thus, it is possible to achieve better temperature uniformity in the BTMS which is the main achievement of the BTMS development. Hence, the direct refrigerant cooling under the evaporation process is recognized as an alternative way to achieve the uniformity of the BTMS temperature. However, this cooling technique still requires an experimental proof and simulation technique for efficient design and temperature uniformity prediction. This is a major research gap and challenge in this research area. Moreover, for a larger scale design, it essentially requires an alternative simulation technique which can simplify the two-phase flow evaporation at the refrigerant tube side cooling. In this case, the heat transfer performance of the two-phase flow evaporation through the refrigerant tube side can be represented by the convective heat transfer coefficient under a certain saturation temperature as supported by many existing papers [26–29]. Hence, the flow evaporation at the refrigerant side can be modeled by

 doi:10.20944/preprints202312.0502.v1

the convective heat transfer mechanism when the h_{ref} is specified. With the convection heat transfer mechanism, the design of the BTMS based direct refrigerant cooling is made possible by finite element method for convection heat transfer. This can help the researchers to develop a larger scale BTMS based refrigerant cooling efficiently. However, from literature surveys, the simulation technique for the BTMS based direct refrigerant cooling via the flow evaporation at the refrigerant side which is represented by the convection heat transfer has not been proposed. Moreover, an experimental proof of it has not been available which is useful for validating the simulated results in which the temperature uniformity under a certain battery heat generation is a major concern. This is a research gap in this research area.

As aforementioned, this present works aims to propose the simulation technique to investigate the cooling performance of the BTMS based direct refrigerant cooling under various operating conditions. The efficient design of the BTMS based direct refrigerant cooling is explored and discussed. The refrigerant side cooling, which is under the two-phase flow evaporation, is simplified to be the convection heat transfer which is represented by the convection heat transfer mechanism (or evaporation heat transfer [30,31]). The developed BTMS-DRC is proposed and the thermal management performance is discussed. The temperature uniformity under various working conditions is explained. The simulation results are validated with the experimental results which were o under the same working conditions. This is to prove the proficiency of the simulation technique. An experimental test bench which is based on dual-evaporators vapor compression refrigeration system is employed to carry out the results for validation. The developed BTMS module (20 cells) is fabricated to examine its cooling performance.

It is found that the BTMS temperature by simulation is close to that by experiment under various working conditions. The discrepancy is around 2.9 – 7.2% depending on the working conditions and heat loads. The simulated results focused on temperature uniformity is also similar to the experimental results. This has confirmed that the proposed simulation technique is developed reasonably and, hence, it can later be used to examine the thermal management performance with a larger scale and other parameters which affect the cooling performance of the BTMS-DRC. These will also be proposed in this work. Even though this paper presents both simulation techniques and experimental proof, the major concern is to employ the simulation techniques for efficiently investigating the performance of BTMS-DRC. The experimental results are only used to validate the simulated results to ensure that the modelling is developed correctly. Full experimental studies of the BTMS-DRC will be proposed in the next publication of the authors.

2. Development of simulation modelling and the experimental setup

2.1. Cycle description and refrigerant flow state based on DE-VCR

As mentioned earlier, the aim of this paper is to demonstrate the thermal management performance of the developed BTMS via direct refrigerant cooling. Hence, the expansion process of the refrigerant from high side to low side pressure is key to thermal performance of the BTMS because the BTMS works as the evaporator. The vapour compression refrigeration system is then employed for this application. Since the BTMS requires a relatively low cooling capacity, a dual-evaporator based vapour compression refrigeration system (DE-VCR) can be applied for this application. Another reason for using it is to demonstrate the refrigeration performance when simultaneously working both air-conditioning and BTMS. A schematic diagram of the system operation is shown in Figure 1.

Preprints (www.preprints.org) | NOT PEER-REVIEWED | Posted: 7 December 2023 doi:10.20944/preprints202312.0502.v1

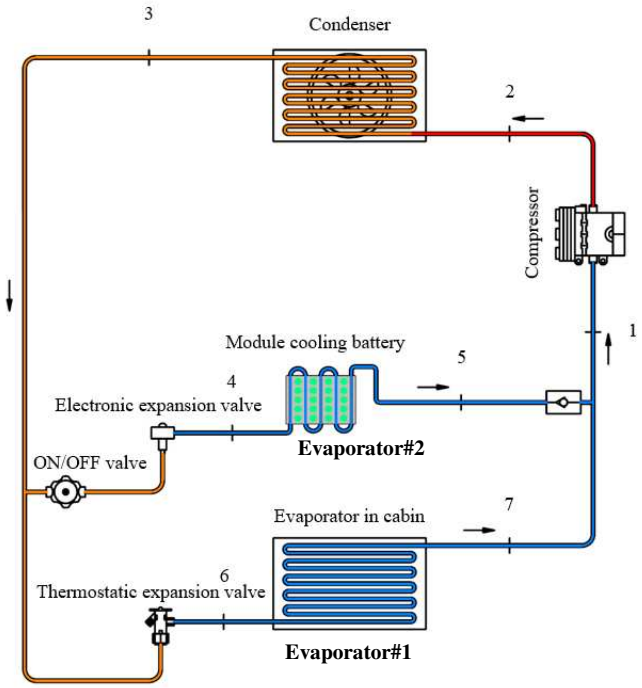

Figure 1. A schematic diagram of dual-evaporator based vapour compression refrigeration system (DE-VCR).

It is seen from Figure 1 that the role of evaporator#1 is to produce cold air for air-conditioning in EVs. Meanwhile, the evaporator#2 works as the BTMS which aims to maintain the module temperature of between 15 and 35 °C depending on the heat generation rate from the battery. During the operation, the low pressure vapour from the two evaporators (state 5 and state 7) is mixed before entering the compressor suction line (state 1). Later, it is compressed via the compressor to produce the superheated vapour at the compressor's discharge (state 2). The superheated vapour is condensed within the condenser by rejecting heat to surroundings. The liquid refrigerant coming out the condenser (state 3) undergoes the expansion process through the expansion valve of each evaporators (state 4 and 5) to complete the cycle operation.

According to the refrigerant flowing through the BTMS, if the refrigerant flow rate is high enough, the flow evaporation of the two-phase fluid will take place within the refrigerant side (small channel or small tubes are mostly used). Hence, the heat transfer from batteries to the refrigerant occurs under the saturated temperatures of the refrigerant as it flows through the BTMS (Evaporator#2). This process comes with the latent heat transfer due to the two-phase refrigerant being evaporated inside. Thus, it is possible to achieve the temperature uniformity on the BTMS which is the main achievement of the BTMS development. Hence, the direct refrigerant cooling under the evaporation process is recognized as an alternative way to achieve the uniformity of the BTMS temperature.

2.2. Development of BTMS based on the direct refrigerant cooling

As explained above, the way to achieve the BTMS temperature uniformity is made possible by means of promoting the flow evaporation of the two-phase refrigerant through the BTMS. Thanks to the refrigerant properties which can evaporate within the small tube or narrow gap, it is feasible to design BTMS with the small flow channels for refrigerant flow which makes an easier solution to apply the refrigerant into the module for promoting the temperatures uniformity and absorbing heat. As a result, the heat transferring area between the refrigerant and modules is as large as possible.

In this work, the battery Li-ion (version 18650) is selected for investigation because it is widely used and provides efficient power capacity. This battery is based on the cylindrical shape. The heat transfer mechanism between the battery and the refrigerant is based on the conduction heat transfer

Preprints (www.preprints.org) | NOT PEER-REVIEWED | Posted: 7 December 2023 doi:10.20944/preprints202312.0502.v1

through the selected solid material which is different from the many published works (mostly based on the convection by air). The problem of water condensation (due to moist air) at relatively low cooling temperatures is relieved (usually the condensation of water occurs at temperatures of below 23 °C under hot and humid climate).

From these reasons, the BTMS is designed as shown in Figure 2 in which twenty five small holes (diameter of 9.525 mm) are made along the length of the main module. The main module is fabricated from aluminum alloy (AA-1060). The battery is installed vertically within the socket as shown in Figure 2. Hence, the height of the module is consistent with the length of battery. The overall size of the BTMS depends on the number of the battery cells. In this present work, the heat generation must be simulated by the battery heat simulator (BHS). It is fabricated from the wired heater which aims to precisely control the heat load for performance assessment. The wired heater is installed within the cylindrical rod which has similar size to the Li-Ion battery (18650). The details of constructing it will be presented in section 2.4 (experimental setup).

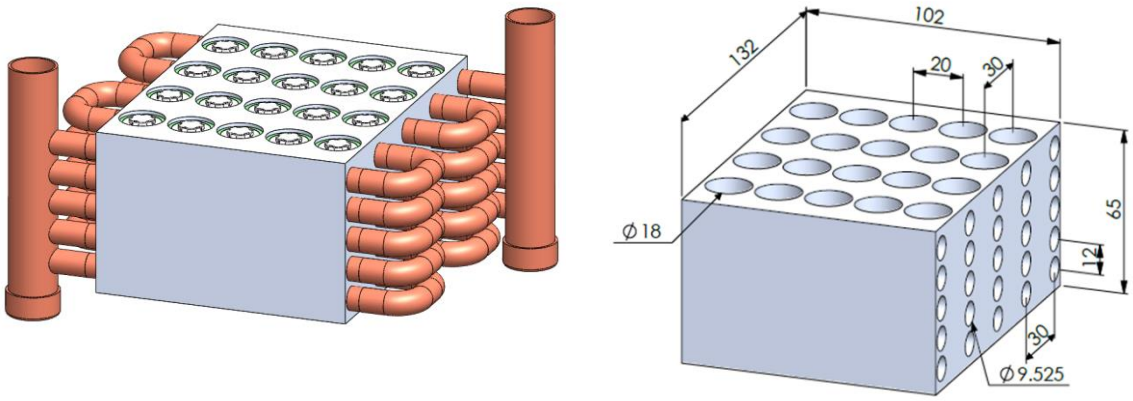

Figure 2. The developed BTMS module.

The cooling performance of the developed BTMS will be investigated to demonstrate the working temperature under various heat generations and operating conditions. The main purpose is to numerically predict the temperature on the module and its temperature uniformity. It is recommended by the previous works [2,3], and [18] that the temperature difference in the module should not be higher than 5 °C and the appropriate working temperature of BTMS must be 15 – 35 °C. These criteria are considered for the cooling performance assessment. The simulation is aimed to employ the numerical techniques to predict the BTMS temperature so that the desired working conditions are satisfactory with the working criteria. Hence, an advantage of the simulation is being able to optimize the desired parameters, cooling capacity, materials used and heat transfer mechanisms.

2.3. Developing the BTMS model for simulation

In this section, the modeling assumptions and strategy for developing the BTMS modeling are explained. The BTMS dimension is based on design criteria proposed in previous section is modeled in the commercial software package, SOLIDWORKS (version 2021 SP3.0.). The procedures to create the physical model and apply the mathematical model are proposed.

2.3.1. Modelling assumptions and working conditions

According to the developed BTMS, the heat is generated at the core of battery and dissipates to the outer surface of the battery which has a certain surface area. Thus, this heat dissipation can simplify to be a constant heat flux for a certain charging or discharging rate. Herein, the battery heat generation is assumed to be the constant heat flux for a certain heat rate. This can support by previous works, Wang et al. [32], Ikramov et al. [33] and Xu et al. [34].

Preprints (www.preprints.org) | NOT PEER-REVIEWED | Posted: 7 December 2023 doi:10.20944/preprints202312.0502.v1

For the refrigerant side cooling, the two-phase fluid enters the small tubes as shown in Figure 2 and, later, it undergoes the evaporation process when absorbing heat from batteries. As explained earlier, the latent heat transfer during the evaporation process is involved. This is made possible when the refrigerant flow rate is adequately high and the expansion pressure ratio through the expansion valve is appropriately regulated. This is to obtain the constant refrigerant temperature due to being operated at the saturated state. The saturation temperature is associated with the pressure during the flow evaporation which is supported by previous works Kim et al. [28], Wang et al. [29] and Ramadan et al. [30]. Also, the flow evaporation of the refrigerant can simplify to be based on the convection heat transfer process as supported by previous works [28–31]. However, it is well known that the two-phase flow phenomenon through the small channels during the evaporation process makes it difficult to correctly develop the simulation models. This is because the non-equilibrium evaporation and heat and mass transfer between phases are involved. Such flow phenomena are very complicated and it is difficult to predict the flow physics accurately. However, from the evaporation heat transfer perspective, the parameter which can represent the convection heat transfer process is the convective heat transfer coefficient. This parameter can be estimated theoretically and can later be proved by experiment (Moon et al. [35] and Li et al. [36]). This makes the evaporation heat transfer prediction more accurate. For this present work, the heat transfer performance and temperature uniformity of the BTMS are the main focuses while the flow characteristics of the two-phase fluid are not a major concern. Therefore, the refrigerant side cooling can simplify to be based on the convection heat transfer mechanism in which the saturation temperature and mass flow rate are key to determine the convective heat transfer coefficient.

The outer surface of the BTMS is designed to be well insulated so that it is independent of the ambient temperature variation. Hence, there is assumed to be no heat loss and gain between the outer surface and surroundings.

2.3.2. Geometries and grid

The geometrical drawings of them are shown in Figure 3. The three-dimensional models (3-D model) of the BTMS modules are created by commercial software, SOLIDWORKS (version 2021 SP3.0.). The dimension is taken from the drawing of the BTMS module. The 3-D model is used to simulate by the finite element method. Hence, the grid elements are generated by software so that all governing equations can be solved numerically. In this work, the grid independent test is also implemented. Herein, three levels of grid elements, coarser (around 39,000), medium (around 99,200) and fine (around 255,000) are created, so that the simulated results (solution) can later be proven to be independent of the number of grid elements (grid independence test). The trigonal-bipyramid is selected for this work which is consistent with the physical problem as supported by [32–34].

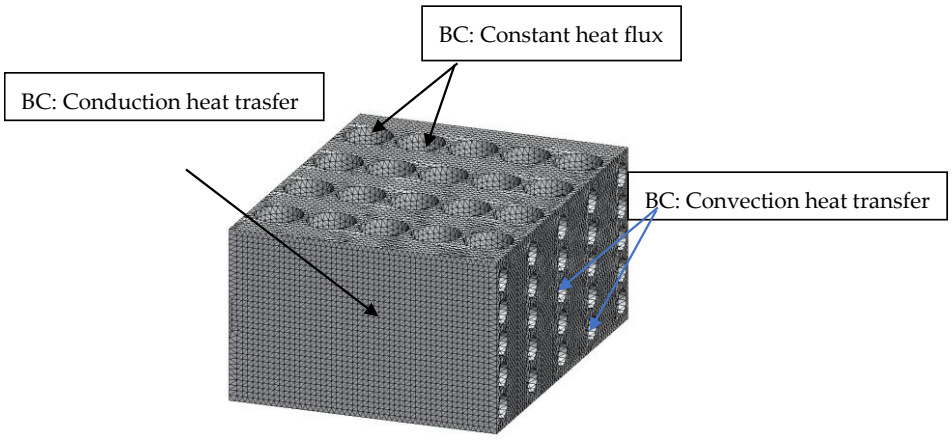

Figure 3. Modelling assumption on the BTMS module.

Preprints (www.preprints.org) | NOT PEER-REVIEWED | Posted: 7 December 2023 doi:10.20944/preprints202312.0502.v1

2.3.3. Heat transfer modeling and boundary conditions

The mathematical model for the heat transfer mechanism based on the conduction and convection is applied to the BTMS models. As explained previously in section 2.1, the refrigerant cooling side is simplified to the evaporation heat transfer which is based on the convection heat transfer model when the evaporation convective heat transfer coefficient is known. Therefore, the finite element method for convection is applied to the refrigerant side. Meanwhile, heat generated by the battery is transferred to the refrigerant by the conduction mechanism. In this case, the heat generated by the battery is assumed to be constant heat flux (the ratio of the heat generation to the surface area of battery). This is to be consistent with the boundary conditions provided by software so that the solution is predicted accurately. The wall surface of the BTMS model is assumed to be well insulated (no heat loss or heat gain).

For the convection heat transfer models, the saturation temperature of the refrigerant and heat transfer coefficient are key to predicting the temperature of the BTMS model. These two parameters are delivered by means of controlling the refrigerant flow rate and evaporation pressure which is the duty of the expansion valve (for practical use). Hence, these parameters can be considered as the control variables for simulations because they are under the control of the investigator. Therefore, the variation of the saturation temperature and heat transfer coefficient will be considered for parametric study. This will be presented in the section 3.

For the heat transfer based on the heat conduction, the thermal conductivity of the selected material is key to produce the working temperature of the BTMS. Hence, the type of materials used is a parameter of interest for this work. In this case, these types of material are considered for parametric study: 1) Silver (k = 490 W/m·K); 2) Copper (k = 380 W/m·K); 3) Aluminum alloy (k =220 W/m·K); 2); 4) Brass (k = 110 W/m·K); 5) Steel (k = 55 W/m·K) and 6) Stainless steel (k = 35 W/m·K).

2.4. Experimental setup

The dual-evaporator based vapour compression refrigeration system test bench was designed and built for investigation. It is used to obtain the experimental results for validation with the simulated results under the same working conditions. The temperatures at the point of interest on the BTMS module are considered for validation. This is to prove the simulation model is developed correctly. The criteria to select the major hardware for constructing the test bench is based on the practical use in EVs. This is to prove that the commercially available hardware can later be adapted for the real use in EVs. The schematic diagram and photograph of the test bench are shown in Figure 4.

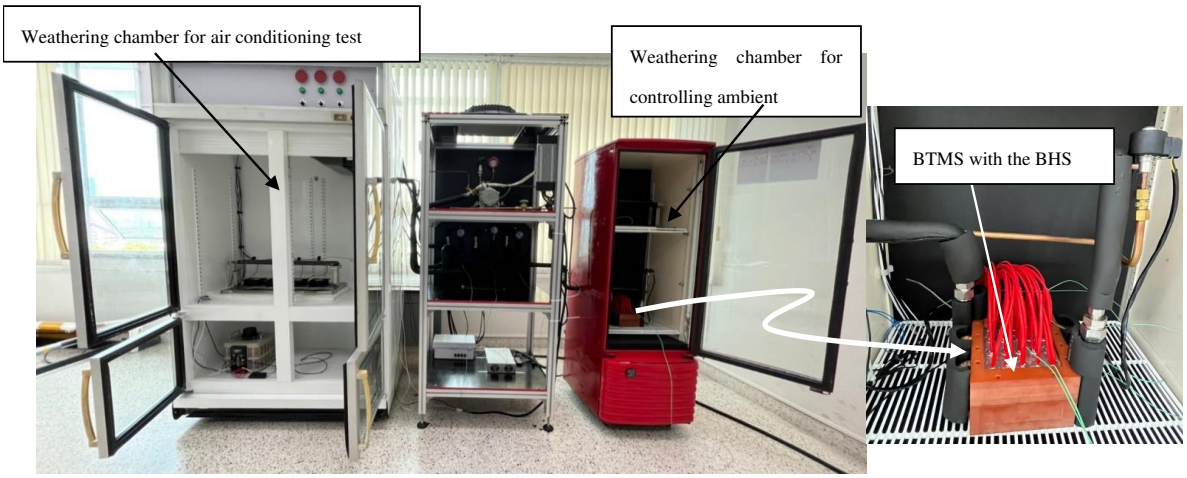

Preprints (www.preprints.org) | NOT PEER-REVIEWED | Posted: 7 December 2023 doi:10.20944/preprints202312.0502.v1

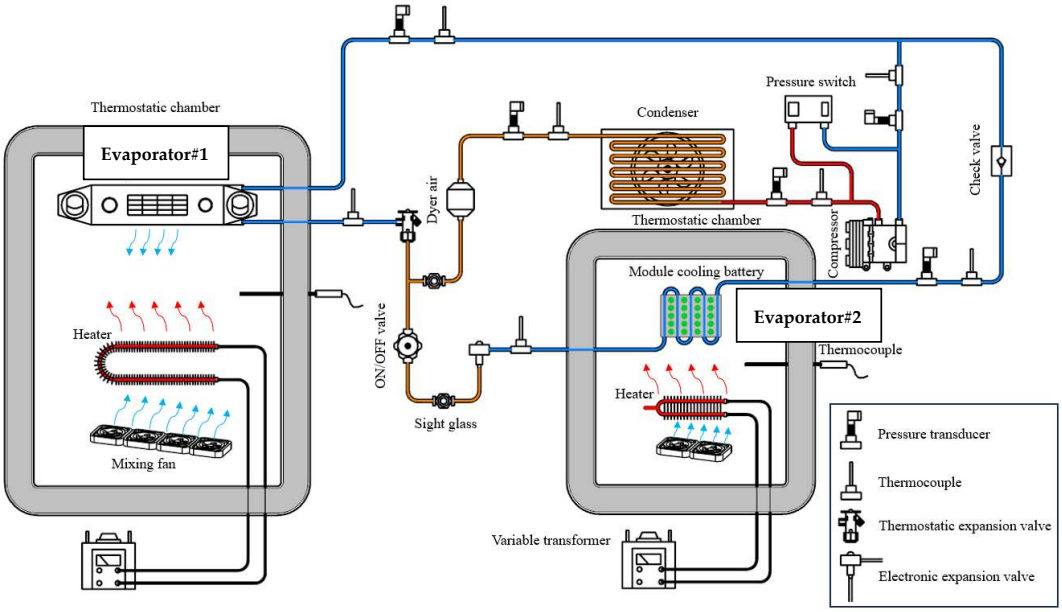

Figure 4. The schematic diagram and photograph of the test bench.

The compressor used has a nominal cooling capacity of 12,000 btu/hr. It is a reciprocating type designed specifically for use in EVs. The compressor is electrically driven by a DC motor with a 24 VDC power supply. The condenser is an air cooled condenser in which the fan speed can be controlled precisely to maintain the condensation pressure at the desired point. This condenser is designed for a common use in conventional automobiles and EVs. The condenser is a mini-channel finned tube heat exchanger.

Evaporator#1 is used to produce cold air for simulating the air-conditioning of EV cabin. It is modified from a commercial automotive fan-coil unit. The fan-coil is installed within the weathering chamber for demonstrating the air-conditioning space. To simulate the cooling load for achieving the thermal comfort conditions, the air heater is installed within the weathering chamber. The heater power is up to 3,000 W and the heat load is controlled precisely by variable transformer (220VAC).

Evaporator#2 is designed to work as the BTMS as explained in previous section. The cooling performance of the BTMS is the main focus of this present work. For efficiently providing the cooling performance assessment of the BTMS, the battery heat simulator (BHS) is fabricated so that the heat generation can be regulated precisely for performance assessment. This is not possible for the real Li-ion battery (version 18650) in which the heat generation varies significantly with the state of charge or discharge. In this work, the shape of the battery heat simulator is designed similar to the real battery whose dimensions are consistent with the battery Li-ion (18650). The wired heater is installed along the axis and thus, the heat generation then dissipates from the core of the BHS to the outer surface which is similar to the real battery. The detailed design of the battery heat simulator is shown in Figure 5.

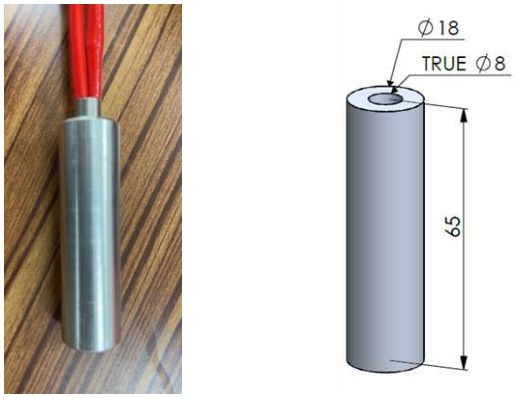

Figure 5. Battery heat simulator (BHS).

Preprints (www.preprints.org) | NOT PEER-REVIEWED | Posted: 7 December 2023 doi:10.20944/preprints202312.0502.v1

A variable transformer (0-220VAC) is used to apply heat load to the BHS. Hence, the steady state operation for heat transfer process can be achieved for further validation with the simulation case. The refrigerant flow rate and the working pressure of the refrigerant side cooling of the BTMS is controlled by means of using the electronic expansion valve (EEV). This allows the desired working pressure and temperature of the BTMS to be controlled precisely.

The temperature at the point of interest is measured by type-k thermocouples. The temperature values are recorded continuously by means of a data logger (Hioki). Hence, transient and steady state operation can be observed clearly. The pressure value at points of interest are detected by a pressure transducer and a pressure gauge which are calibrated before being installed into the test bench.

The air-conditioning space temperature (evaporator#1) can be controlled precisely to achieve the thermal comfort conditions (25 °C and 50%RH). The PID controller together with a solid-state relay is used to regulate the heater power of the air-heater. Hence, the heat load can be varied to obtain the constant air-conditioning space temperature.

The condensation pressure of the condenser is regulated precisely. This is made possible by controlling the fan-speed of the air-cooled condenser. Hence, the condensation pressure can be controlled at the desired point for assessments.

3. Results and discussions

3.1. Validations of the results and proof of temperature uniformity of BTMS-DRC

This section aims to demonstrate the proficiency in predicting the BTMS module temperature via the proposed simulation technique and to demonstrate the temperature uniformity on the module which is based on the proposed design criteria. The experimental results and simulated results determined under the same working condition are compared and shown in Table 1. The module temperatures at the point of interest as shown in Figure 6 are considered for comparison to indicate the accuracy in predicting temperature via simulations. The comparison is implemented under various total battery heat generations ranging from 100 to 300 W for ensuring that the simulation technique is developed correctly.

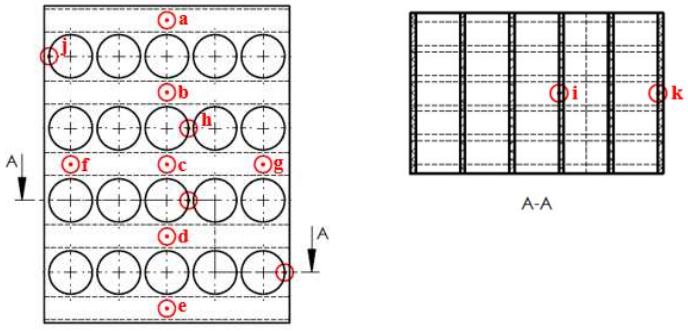

Figure 6. The points of interest on the BTMS module for validations.

Table 1. Comparisons of the simulated module temperature with those of experiements .

Point	Heat generation 100 W			Heat generation 200 W			Heat generation 300 W		
	T_{sim}	T_{EXP}	%error	T_{sim}	T_{EXP}	%error	T_{sim}	T_{EXP}	%error
a	10.5	10.2	2.9	17.6	16.8	4.5	26.7	25.8	3.4
b	11.1	10.4	6.3	18.8	17.6	6.4	28.5	26.7	6.3
c	11.3	10.5	7.1	19.2	18.4	4.2	29.1	27.2	6.5
d	11.1	10.3	7.2	18.8	17.5	6.9	28.5	26.6	6.7
e	10.5	10.1	3.8	17.6	16.7	5.1	26.7	25.8	3.4
f	11.2	10.4	7.1	19.0	18.2	4.2	28.8	26.9	6.6
g	11.2	10.4	7.1	19.0	18.2	4.2	28.8	26.9	6.6

 doi:10.20944/preprints202312.0502.v1

h	11.4	10.8	5.3	19.3	18.7	3.1	29.2	28.3	3.1
i	11.4	10.7	6.1	19.3	18.6	3.6	29.2	28.3	3.1
j	10.1	9.5	5.9	17.0	16.3	4.1	25.9	24.3	6.2
k	10.1	9.4	6.9	17.0	16.2	4.7	25.9	24.3	6.2

Table 1 and Figure 6 depict the comparisons of the module temperatures for the points of interest in the module which show that the simulated temperature in the module (point a – k) is close to the experimentally measured temperature. The experimental results are slightly lower than the simulated results under the same working condition. The obtained error is around 2.9 - 7.2%, depending on the working condition. This indicates that the simulated result based on the proposed simulation technique agrees well with the experimental results. It also shows that the simulated temperature at point a – e (representing the temperature at the middle of the module) is slightly higher than other points (point f – k). This is also in good agreement with the experiment. It is clearly seen that the difference in temperatures in the module is around 1.2 – 3.7 °C (both simulation and experiment) depending on the working conditions. This meets the requirement for the Li-ion battery which recommends that the difference in temperature between cells should not exceed 5 °C. It has proven that the proposed cooling technique (direct refrigerant cooling based on the flow evaporation) is a way to provide the efficient temperature uniformity on the BTMS which is better than that proposed by the previous works which were based on the air-cooling and water-cooling [14–18].

Alternatively, the temperature contour obtained from simulation is employed to demonstrate the temperature uniformity on the module which is shown in Figure 7. It is seen from the contour that the highest temperature is located at the middle of the module. However, the difference in temperatures in the module is around 1.7 – 3.7 °C which is lower than the appropriate working condition for Li-ion battery. It is also seen that at the section A-A and B-B, which represent the temperature inside the material used for constructing the module, the temperature is uniform which is consistent with that of the experimental measurement. This can ensure that the proposed BTMS-DRC is in good quality (both working temperature and temperature uniformity).

The major reason of producing the temperature uniformity is that the flow evaporation of the refrigerant through the small tubes causes the refrigerant temperature to remain constant. Hence, the state of the refrigeant is under the saturated condition. Thus, there is not much difference in temperature at the refrigerant tube side cooling due to being operated with the saturation temperature. This causes the module temperature to be more uniform than in other cooling techniques as proposed in previous work [18–22]. Therefore, this paper provides the alternative cooling technique and simulation techniques for predicting temperature which has not been available from open literature.

Validations of the results have shown that the proposed simulation technique can efficiently be used to predict the module temperature based on the direct refrigerant cooling. This is an effective tool to design the BTMS based direct refrigerant cooling. The cooling performance of the proposed direct refrigerant cooling technique has been proven to be an efficient way to improve the BTMS for Li-Ion battery. It has also shown that the proposed simulation method for predicting temperature on the BTMS is in good agreement with the experimental results. This provides an advantage in investigating the impact of the other parameters, heat generation and module's geometry on the thermal management performance. This will be presented later in the next section.

Preprints (www.preprints.org) | NOT PEER-REVIEWED | Posted: 7 December 2023 doi:10.20944/preprints202312.0502.v1

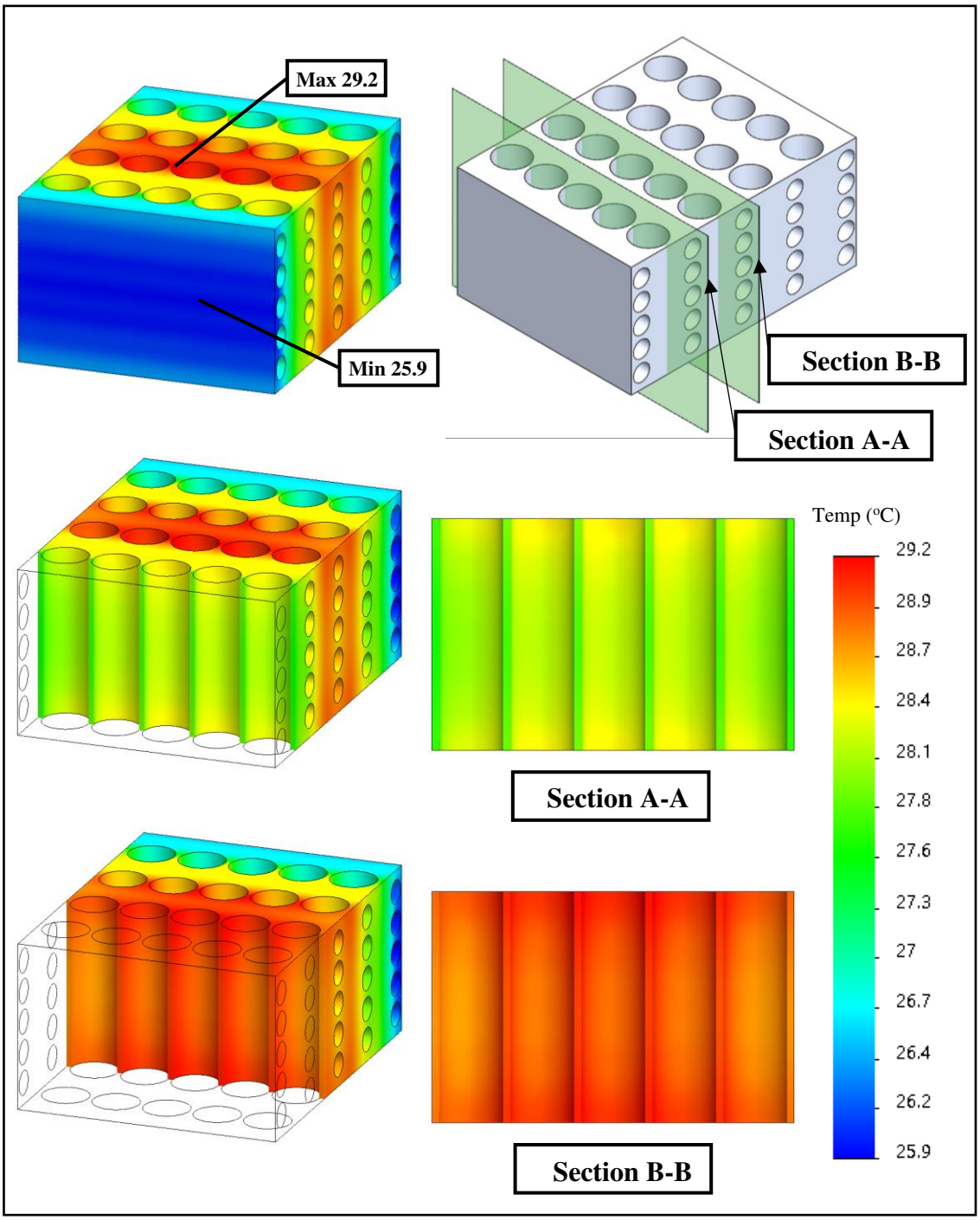

Figure 7. The temperature contour of the module.

3.2. Influence of heat generations

To investigate this, the temperature at the refrigerant tube side is fixed at 10 °C. The total heat generation is increased from 80 to 320 W which aims to demonstrate the module temperature under various heat rates. The convection heat transfer coefficient for simulation is fixed at different values ranging from 200 to 300 W/m²·k which is consistent with the flow Reynold number at the refrigerant tube side for the evaporation process within the small tube [26–28]. Figure 8 shows the simulated temperature at the middle of the module and Figure 9 shows the temperature contour of the module under a heat generation of 160 W, 220 W and 320 W, respectively.

Preprints (www.preprints.org) | NOT PEER-REVIEWED | Posted: 7 December 2023 doi:10.20944/preprints202312.0502.v1

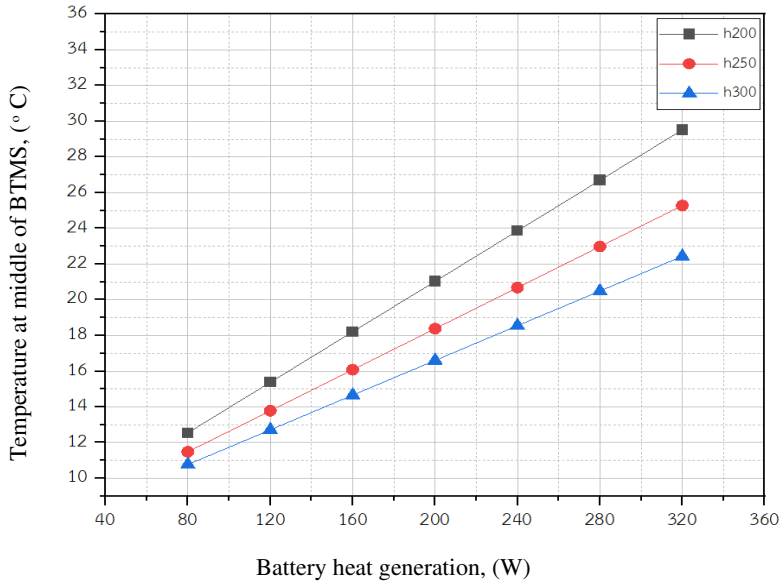

Figure 8. The module temperature against the heat generations.

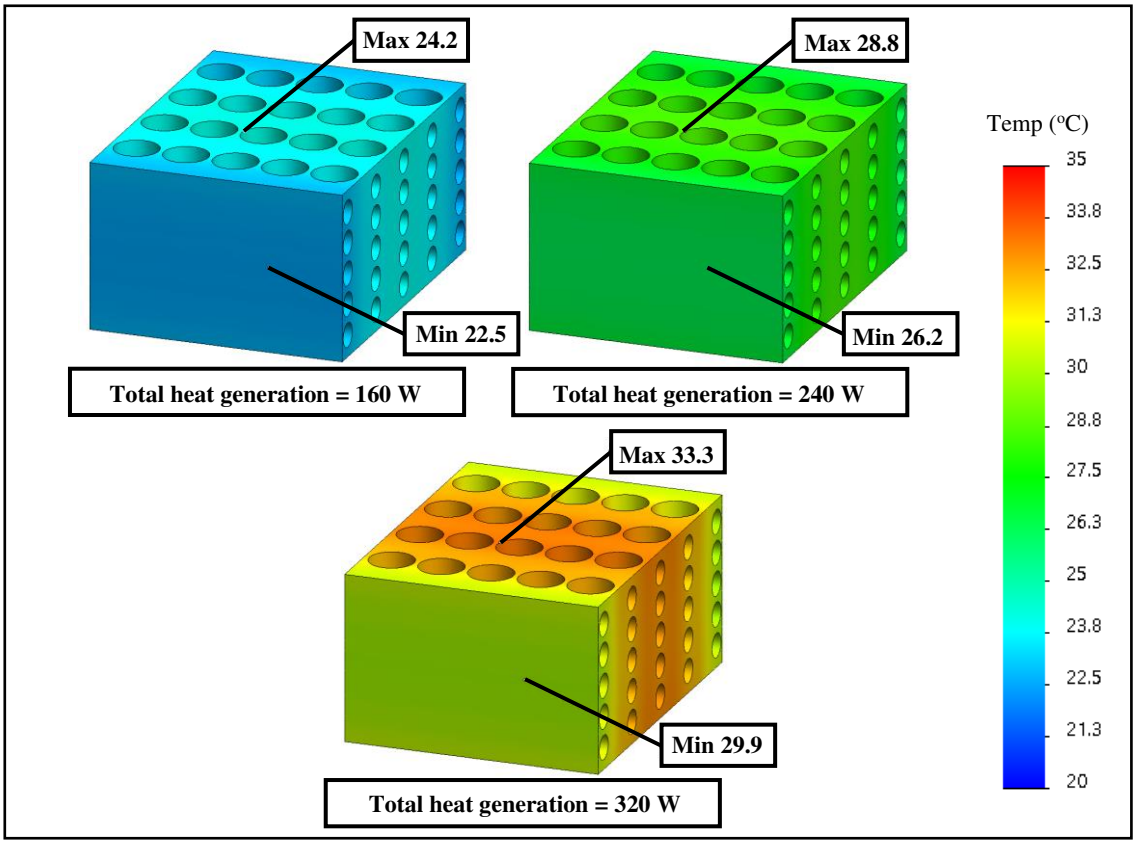

Figure 9. The temperature contours of the BTMS when varying the heat generation.

It is seen from Figure 8 that for a certain h_{ref} , the module temperature increases when increasing the heat generation. It is clearly seen that throughout the range of the specified heat generation and h_{ref}, the module temperature is lower than 30 °C, which is still below the maximum working temperature for Li-ion battery. It can also be seen that the module temperature at a certain heat generation decreases when the value of h_{ref} is increased. In practice, the value of h_{ref} depends significantly on the refrigerant flow rate. This means the mass flow rate of the refrigerant plays a crucial role in the module temperature. Hence, a careful design of the BTMS based direct refrigerant

Preprints (www.preprints.org) | NOT PEER-REVIEWED | Posted: 7 December 2023 doi:10.20944/preprints202312.0502.v1

cooling should focus on the h_{ref}. This present work will provide the impact of the h_{ref} which will later be presented in section 3.4.

Figure 9 illustrates the contour of the module temperature when increasing the heat generation. It is clearly seen that even though the temperature is increased with heat generation, the temperature difference on the module is around 1.7 – 4.2 °C which is lower than the recommended value for Li-ion. This indicates the efficient cooling performance via the proposed design criteria. This is because it produces a sufficient temperature uniformity even when the heat load is increased. This has guaranteed that the BTMS based direct refrigerant cooling proposed in this work can be recognized as the efficient cooling method.

3.3. Influence of the thermal conductivity

This section aims to demonstrate how the thermal conductivity of the material affects the module temperature. This is to demonstrate the ability to perform the conduction heat transfer. It will significantly affect the module temperature even when the heat transfer rate (battery heat generation) is identical.

To investigate this, the total heat generation is fixed at 300 W while the saturation temperature of the refrigerant side cooling is 10 °C. The convection heat transfer coefficient is held constant at 250 W/m²·K. The considered materials for investigations are copper (k = 250 W/m·K), brass (k = 122 W/m·K), aluminum alloy (k = 211 W/m·K), steel (k = 55 W/m·K) and stainless steel (k = 35 W/m·K). The simulated results (the module temperature) at the middle are tabulated in Table 2. To demonstrate the ability to produce the temperature uniformity of the modulethe temperature contour is used for comparisons. This is shown in Figure 10.

It is seen from Table 2 that the material which has a relatively high thermal conductivity (silver, aluminum alloy, brass, copper) can produce a lower module temperature (T_{mid}) than that of a relatively low thermal conductivity (steel and stainless steel) under the same working condition. This is due to the fact that a higher thermal conductivity can perform heat transfer faster. This causes the accumulated heat within the material under a certaintime interval to become lower which yields a lower module temperature. It is noticeable that the steel and stainless steel are not recommended for this application due to providing poor cooling performance and working temperature.

Table 2. The type of materials used, thermal conductivity and the BTMS temperature (T_{mid}/T_{min}).

Materials	k (W/m·K)	T_{mid}	T_{min}	$\Delta T_{mid/min}$
Silver	430	28.5	26.4	1.9
Copper	390	28.6	26.8	1.8
Aluminum Alloy-1060	215	29.2	25.9	3.3
Brass	110	30.2	25.1	4.1
Steel	45	34.5	21.1	**13.4**
Stainless Steel	15	38.2	18.4	**19.8**

Preprints (www.preprints.org) | NOT PEER-REVIEWED | Posted: 7 December 2023 doi:10.20944/preprints202312.0502.v1

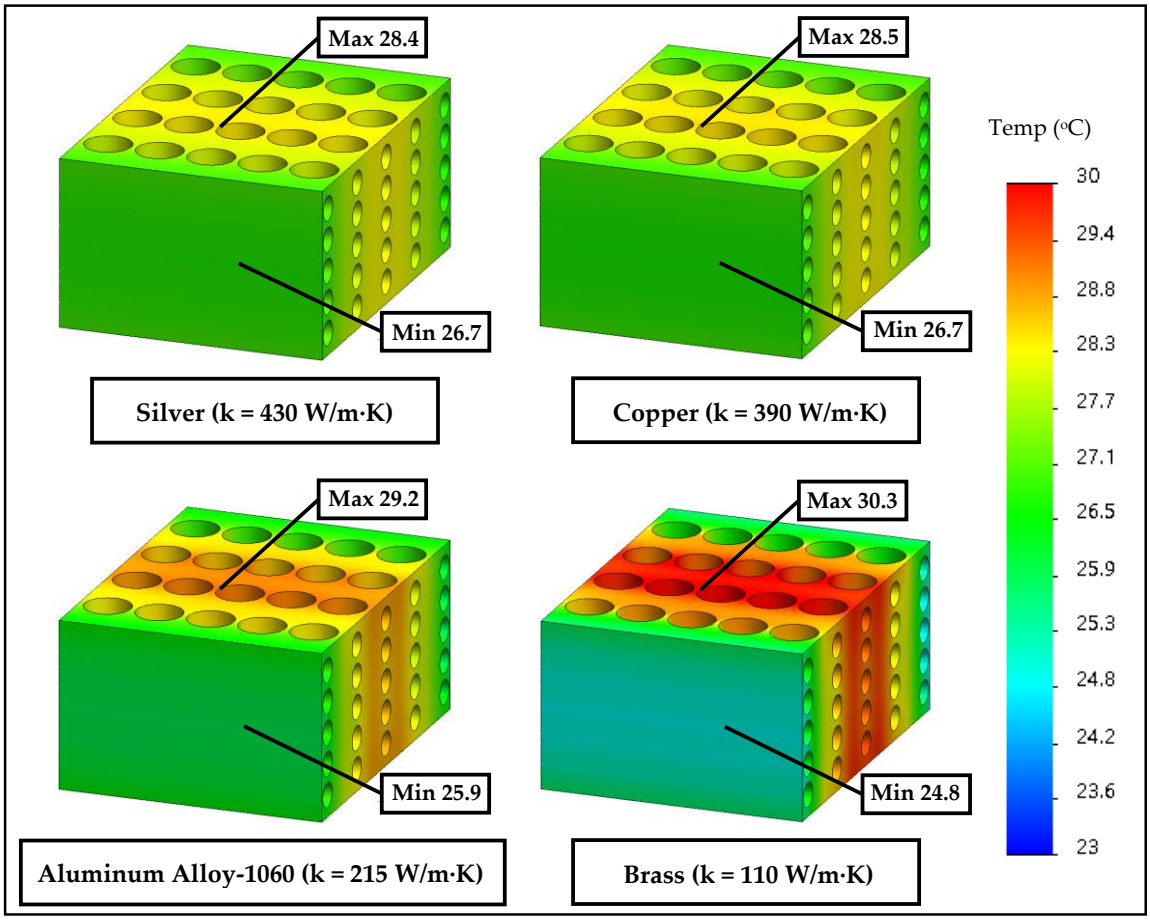

Figure 10. The temperature contours of the BTMS when changing the material used.

When considering the ability to produce the temperature uniformity seen from the contour temperature in Figure 10, the material which has a relatively high thermal conductivity can produce more uniform temperatures in the module as seen in Table 3 ($\Delta T_{mid/min}$). It is clearly seen that the $\Delta T_{mid/min}$ of the silver, copper, aluminum alloy and brass meets the requirement for working with the Li-ion battery because the difference in temperature between cells is below 5 °C. Meanwhile, steel and stainless steel show a very poor thermal mangement performance because the accumualted heat within the material is quite high due to a poor heat tranfer process. This causes the module temperature to quite high and the non-uniformity of the module temperature.

However, for the material which has high thermal conductivity, there is not much difference in ability to produce the temperature uniformity. This means that as long as the working temperature of the Li-ion battery is below the maximum working temperature and the acceptable temperature uniformity, the selected material for constructing the module should be compromised. This is because the construction cost is an important factor for demonstrating the worth construction.

3.2. Influence of the convective heat transfer coefficients

As explained earlier, the key to perform convection heat transfer process under the flow evaporation of the refrigerant is represented by the convection heat transfer coefficient of the refrigerant (h_{ref}). In practice, the h_{ref} depends significantly on the refrigerant flow rate and saturated working condition of the refrigerant which is under the control of the researchers. This will significantly affect the Reynold number, Prandth number [26,27,37–39], resulting in the variations of the h_{ref}. Hence, this section aims to demonstrate how the variations in the h_{ref} affects the BTMS temperature.

Preprints (www.preprints.org) | NOT PEER-REVIEWED | Posted: 7 December 2023 doi:10.20944/preprints202312.0502.v1

To demonstrate this, the refrigerant saturation temperature is maintained at 7 °C. The convection heat transfer coefficient is varied ranging from 80 to 400 W/m²·K. The total battery heat generation is fixed at different values ranging from 40 to 120 W which corresponds with the heat flux of 544.1 W/m² to 1,632.4 W/m².

Figure 11 depicts the temperature at the middle of the BTMS module against the variation of h_{ref}. It is also seen that the module temperature decreases sharply with increasing the h_{ref}, however; the module temperature decreases slightly when h_{ref} is higher than a ceratain value. For example, for a particular heat generation of 120 W, the module temperature drops from 28.5 to 12.8 °C when h_{ref} increases from 80 to 280 W/m²·K. Later, the module temperature drops from 12.8 to 11.2 °C (slightly decreases) when h_{ref} increases from 280 to 400 W/m²·K.

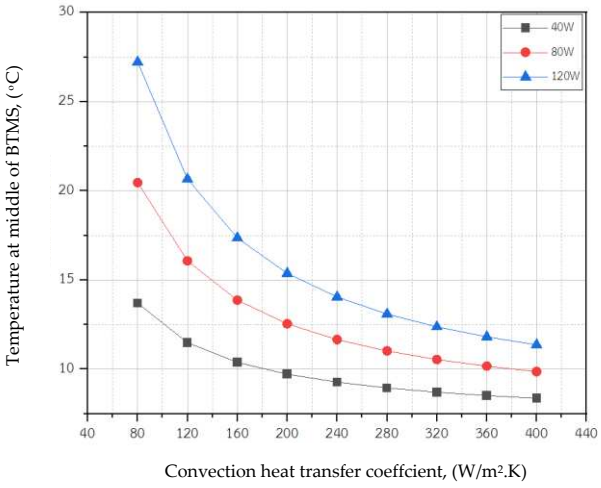

Figure 11. The module temperature against the heat transfer coefficient.

At relatively low h_{ref}, the ability to produce heat transfer performance is not good even when the refrigerant saturation temperature is kept at 7 °C (quite low). This is mainly the cause of the h_{ref} value not being high enough. The reason for this is that the refrigerant mass flow rate is too low to produce the best possible evaporation heat transfer. For this reason, the heat generated by batteries is accumulated within the BTMS module which results in the module temperature increasing when h_{ref} decreases.

It can also be seen that for a certain h_{ref} , when the battery heat generation is increased, the BTMS module temperature is increased. This is due to the fact that the refrigerant flow rate is kept constant at a certain value and, hence, the heat transfer process is occurred by means of a larger temperature difference. This causes the module temperature to increase. It is obviously seen that when the h_{ref} is higher than 240 W/m²·K, the BTMS temperature is slightly decreased. This means if the h_{ref} is too high, it will not give advantage to the heat transfer process. This implies that it is not necessary to promote a quite high refrigerant flow rate through the module which provides positive impact for practical operation (energy savings). The reason is that at quite high h_{ref}, a better heat transfer process is the result. Hence, the BTMS temperature can be as low as possible. The h_{ref} must be properly applied for performing the thermal management of the battery module. Therefore, in practice, the refrigerant flow rate must be regulated properly. This is made possible when the EEV is controlled precisely. However, the changes in the flow rate by means of the EEV or other expansion valves sometimes produce different refrigerant saturation temperature due to the change in the valve pressure ratio. This effect also results in varying the h_{ref}. It will be discussed in the next section.

3.4. Effect of refrigerant saturation temperature

As discussed earlier, the saturation temperature of the refrigerant can be regulated by adjusting the expansion pressure ratio of the expansion valve together with the proper selection of the valve

Preprints (www.preprints.org) | NOT PEER-REVIEWED | Posted: 7 December 2023 doi:10.20944/preprints202312.0502.v1

orifice. Hence, the refrigerant saturation temperature is considered to be a variable parameter for investigating the cooling performance based on the flow evaporation. This section provides the discussion on the impact of the refrigerant saturation temperature. In this investigation, the h_{ref} is fixed at 250 W/m^2·K while the refrigerant saturation temperature is varied ranging from 4 to 26 °C. In addition, the simulation is implemented under various battery heat generations which is ranged from 40 to 120 W. The simulated temperatures in the BTMS-DRC module are depicted in Figure 12.

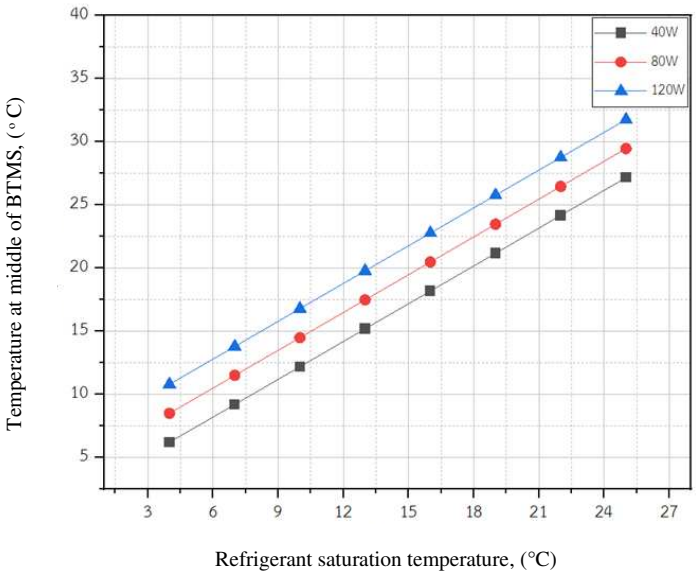

Figure 12. The module temperature against the refrigerant saturation temperature.

It is seen from Figure 12 that for a certain cooling load, the module temperature is increased when increasing the refrigerant saturation temperature. This means increasing the refrigerant saturation temperature mitigates its ability to produce cooling temperatures (module temperature). However, throughout the range of the specified working condition, the module temperature is below the upper limit of the appropiate working temperature (below 35 °C). Usually, if the refrigeration system is operated with a higher evaporating temperature (BTMS works as the evaporator), the system COP will increase which leads to a decrease in the electricity consumption for the compressor. Therefore, for a certain heat generation, the working saturation tmeprature at the refrigerant tube side cooling should be as high as possible. However, it is consistent with the recommended working temperature for Li-ion. Hence, the module temperature is a key to select the working refrigerant saturation temperature.

It is also found from Figure 12 that for a certain refrigerant saturation temperature, the module temperature is increased with an increase in the battery heat generation. This is because the refrigerant must absorb more heat load under a fixed h_{ref} which causes a larger differential temperature between the refrigerant and module. Hence, the module temperature is then increased when increasing the heat generation under the same saturation temperature.

As discussed above, for the efficient design of the BTMS-DRC, the saturation temperature of the refrigerant tube side cooling is a significant parameter for consideration. This is because it dominants the cycle efficiency which results in a reduction of the electricity consumption. The results have shown that the change in the refrigerant saturation temperature causes a significant variations of the module temperature. For a certain heat generation, and as long as the module temperature is below 35 °C, the refrigerant saturation temperature should be as high as possible.

4. Conclusions

This paper proposed an alternative simulation technique for an efficient design and parametric studies of the BTMS based direct refrigerant cooling. The finite element method of heat transfer (convection and conduction) was applied to simulate the developed BTMS module. The refrigerant

 doi:10.20944/preprints202312.0502.v1

side cooling was based on the convection heat transfer mechanism while the conduction heat transfer mechanism was applied to the main module. The simulated results were validated with the experimental results obtained from the test bench. The major findings of this paper can be summarized as follows:

- The simulated results (the module temperature) via the simulation agreed well with the experimental results. It was also found that the simulated results remained close to that experimental results when varying the operating conditions. The error from validation was around 2.9 – 7.2%.
- The simulated results also agreed well with the experimental results when focusing on the temperature uniformity of the module. The difference in temperature in the module did not exceed 5 °C (both simulations and experiments). This has shown that the BTMS-DRC is an alternative way to achieve the sufficient temperature uniformity. This is due to the advantages of the two-phase flow evaporation.
- For the parametric investigation via simulations, an increase in the battery heat generation caused the module temperature to increase. Therefore, the heat generation for indicating the working capacity of the BTMS must be consistent with the appropriate working temperature for Li-ion battery.
- For emphasizing the heat transfer mechanism, it was evident that the change in the convection heat transfer coefficient significantly affected the module temperature. Using a too low h_{ref} resulted in producing a quite high module temperature. On the other hand, using a too high h_{ref} has less impact on producing the lowest module temperature. This has shown that the h_{ref} for design the BTMS-DRC must be carefully considered.
- Additionally, the change in the refrigerant saturation temperature significantly affected the module temperature even when the h_{ref} was held constant. The investigation indicated that for a certain heat generation and h_{ref}, the refrigerant saturation temperature should be as high as possible. This can provide an advantage to the refrigeration system.

Hopefully, the simulation technique and parametric investigation proposed in this paper is useful for a better understanding of the direct refrigerant cooling mechanisms and efficiently designing the BTMS-DRC. The validation of the results has confirmed that the proposed simulation technique is developed reasonably. This is an alternative tool for designing a larger scale BTMS-DRC. The full experimental investigation on the BTMS-DRC under various working conditions will be provided in the next publication of the authors.

Author Contributions: "Conceptualization, S.J., S.C., and T.T.; methodology, S.J., S.C., and T.T..; software, S.J., S.C., K.S. and T.T.; validation, S.J., S.C., K.S. and T.T.; formal analysis, S.J., S.C., K.S. and T.T.; investigation, S.J., S.C. and T.T.; data curation, S.J., S.C., K.S. and T.T.; writing—original draft preparation, S.J., S.C., K.S. and T.T.; writing—review and editing, S.J., S.C., K.S. and T.T.; supervision, S.C., K.S. and T.T.; funding acquisition, S.J., S.C., K.S. and T.T. All authors have read and agreed to the published version of the manuscript.

Funding: This research was funded by National Science, Research and Innovation Fund (NSRF) and King Mongkut's University of Technology North Bangkok with Contract no. KMUTNB-FF-66-15.

Data Availability Statement: Not applicable.

Acknowledgments: This research was funded by National Science, Research and Innovation Fund (NSRF) and King Mongkut's University of Technology North Bangkok with Contract no. KMUTNB-FF-66-15. The first author would like to thank the Sirindhorn International Thai-German Graduate School of Engineering (TGGS), King Mongkut's University of Technology North Bangkok for offering the academic sponsorship.

Conflicts of Interest: The authors declare no conflict of interest

Nomenclature

AC	Alternating current
ARAC	Advanced refrigeration and air conditioning laboratory

 doi:10.20944/preprints202312.0502.v1

BC	Boundary conditions
BTMS	The battery thermal management system
BHS	Battery heat simulator
COP	Coefficient of performance
DC	Direct current
DE-VCR	Dual-evaporator based vapour compression refrigeration system
DRC	Direct refrigerant cooling
EEV	Electric expansion valve
EVs	Electric vehicles
h_{ref}	Convection heat transfer coefficient at the refrigerant side
k	Thermal conductivity
PID	Proportional integral derivative
RH	Relative humidity
T_{exp}	Experimental temperature
T_{max}	Maximum temperature
T_{mid}	Middle temperature
T_{min}	Minimum temperature
T_{sim}	Simulation Temperature

References

1. Ke, Q., Li, X., Guo, J., Cao, W., Wang, Y. and Jiang, F., 2022. The retarding effect of liquid-cooling thermal management on thermal runaway propagation in lithium-ion batteries. Journal of Energy Storage, 48, p.104063.
2. Sun, Z., Guo, Y., Zhang, C., Xu, H., Zhou, Q. and Wang, C., 2022. A novel hybrid battery thermal management system for prevention of thermal runaway propagation. IEEE Transactions on Transportation Electrification.
3. Liu, J., Chavan, S. and Kim, S.C., 2023. Investigation of the Electrochemical and Thermal Characteristics of NCM811-21700 Cylindrical Lithium-Ion Battery: A Numerical Study and Model Validation. Energies, 16(17), p.6407.
4. Azzopardi, B., Hapid, A., Kaleg, S., Onggo, D. and Budiman, A.C., 2023. Recent Advances in Battery Pack Polymer Composites. Energies, 16(17), p.6223.
5. Hong, J., Wang, Z., Qu, C., Zhou, Y., Shan, T., Zhang, J. and Hou, Y., 2022. Investigation on overcharge-caused thermal runaway of lithium-ion batteries in real-world electric vehicles. Applied Energy, 321, p.119229.
6. Olabi, A.G., Maghrabie, H.M., Adhari, O.H.K., Sayed, E.T., Yousef, B.A., Salameh, T., Kamil, M. and Abdelkareem, M.A., 2022. Battery thermal management systems: Recent progress and challenges. International Journal of Thermofluids, 15, p.100171.
7. Luo, J., Zou, D., Wang, Y., Wang, S. and Huang, L., 2022. Battery thermal management systems (BTMs) based on phase change material (PCM): A comprehensive review. Chemical Engineering Journal, 430, p.132741.
8. Xu, J., Zhang, C., Wan, Z., Chen, X., Chan, S.H. and Tu, Z., 2022. Progress and perspectives of integrated thermal management systems in PEM fuel cell vehicles: A review. Renewable and Sustainable Energy Reviews, 155, p.111908.
9. Chen, W.Y., Shi, X.L., Zou, J. and Chen, Z.G., 2022. Thermoelectric coolers for on-chip thermal management: Materials, design, and optimization. Materials Science and Engineering: R: Reports, 151, p.100700.
10. Fan, H., Wang, L., Chen, W., Liu, B. and Wang, P., 2023. A J-Type Air-Cooled Battery Thermal Management System Design and Optimization Based on the Electro-Thermal Coupled Model. Energies, 16(16), p.5962.

11. Akinlabi, A.H. and Solyali, D., 2020. Configuration, design, and optimization of air-cooled battery thermal management system for electric vehicles: A review. Renewable and Sustainable Energy Reviews, 125, p.109815.
12. Wang, M., Teng, S., Xi, H. and Li, Y., 2021. Cooling performance optimization of air-cooled battery thermal management system. Applied thermal engineering, 195, p.117242.
13. Chen, K., Song, M., Wei, W. and Wang, S., 2019. Design of the structure of battery pack in parallel air-cooled battery thermal management system for cooling efficiency improvement. International Journal of Heat and Mass Transfer, 132, pp.309-321.
14. Jouhara, H., Serey, N., Khordehgah, N., Bennett, R., Almahmoud, S. and Lester, S.P., 2020. Investigation, development and experimental analyses of a heat pipe based battery thermal management system. International Journal of Thermofluids, 1, p.100004.
15. Kalaf, O., Solyali, D., Asmael, M., Zeeshan, Q., Safaei, B. and Askir, A., 2021. Experimental and simulation study of liquid coolant battery thermal management system for electric vehicles: A review. International Journal of Energy Research, 45(5), pp.6495-6517.
16. Qaderi, A. and Veysi, F., 2022. Investigation of a water-NEPCM cooling thermal management system for cylindrical 18650 Li-ion batteries. Energy, 244, p.122570.
17. Siruvuri, S.V. and Budarapu, P.R., 2020. Studies on thermal management of Lithium-ion battery pack using water as the cooling fluid. Journal of Energy Storage, 29, p.101377.
18. Gao, R., Fan, Z. and Liu, S., 2022. A gradient channel-based novel design of liquid-cooled battery thermal management system for thermal uniformity improvement. Journal of Energy Storage, 48, p.104014.
19. Hong, S.H., Jang, D.S., Park, S., Yun, S. and Kim, Y., 2020. Thermal performance of direct two-phase refrigerant cooling for lithium-ion batteries in electric vehicles. Applied Thermal Engineering, p.115213.
20. Wang, Y.F. and Wu, J.T., 2020. Thermal performance predictions for an HFE-7000 direct flow boiling cooled battery thermal management system for electric vehicles. Energy Conversion and Management, 207, p.112569.
21. Cen, J. and Jiang, F., 2020. Li-ion power battery temperature control by a battery thermal management and vehicle cabin air conditioning integrated system. Energy for Sustainable Development, 57, pp.141-148.
22. Gillet, T., Andres, E., El-Bakkali, A., Lemort, V., Rulliere, R. and Haberschill, P., 2018. Sleeping evaporator and refrigerant maldistribution: An experimental investigation in an automotive multi-evaporator air-conditioning and battery cooling system. International Journal of Refrigeration, 90, pp.119-131.
23. Ren, H., Jia, L., Dang, C., Yang, C., Jia, H. and Liu, J., 2022. Experimental investigation on pouch lithium-ion battery thermal management with mini-channels cooling plate based on heat generation characteristic. Journal of Thermal Science, 31(3), pp.816-829.
24. Chen, Z., Yang, S., Pan, M. and Xu, J., 2022. Experimental investigation on thermal management of lithium-ion battery with roll bond liquid cooling plate. Applied Thermal Engineering, 206, p.118106.
25. Cao, C., Xie, L., He, X., Ji, Q., Zhao, H. and Du, Y., 2022. Numerical study on the flow and heat-transfer characteristics of horizontal finned-tube falling-film evaporation: Effects of liquid column spacing and wettability. International Journal of Heat and Mass Transfer, 188, p.122665.
26. Jatau, T. and Bello-Ochende, T., 2022. Numerical investigation and entropy generation for flow boiling evaporation in U-bend tube heat exchanger with elliptical and circular cross-sections. Thermal Science and Engineering Progress, 35, p.101480.
27. Du, S., Li, Q., Cao, X., Song, Q., Wang, D., Li, Y., Li, L. and Liu, J., 2022. Investigation on heat transfer and pressure drop correlations of R600a air-cooled finned tube evaporator for fridge. International Journal of Refrigeration, 144, pp.118-127.
28. Kim, C.H. and Kim, N.H., 2022. Evaporation heat transfer and pressure drop of low GWP R-404A alternative refrigerants in a multiport tube. International Journal of Heat and Mass Transfer, 184, p.122386.
29. Wang, X., Kukulka, D.J., Liu, X.Z., Feng, W., Wang, X.B., Li, W. and Wang, Z.P., 2023. Evaporation Flow Heat Transfer Characteristics of Stainless Steel and Copper Enhanced Tubes. Energies, 16(5), p.2331.
30. Ramadan, Z., Park, K.Y. and Park, C.W., 2022. Numerical and experimental investigation of heat and mass transfer performance of pool boiling type shell and plate evaporator. International Journal of Heat and Mass Transfer, 199, p.123428.
31. Chen, X., Sheng, J., Lu, T., Wang, J., Zhang, K. and Chen, X., 2022. Three-dimensional heat transfer coefficient distributions in horizontal tube falling film evaporation. Applied Thermal Engineering, 216, p.119141.

32. Wang, K.X., Zhou, E.L., Wei, B.L., Wu, Y. and Wang, G., 2022. An efficient and accurate numerical method for the heat conduction problems of thermal metamaterials based on edge-based smoothed finite element method. Engineering Analysis with Boundary Elements, 134, pp.282-297.
33. Ikramov, A., Polatov, A., Pulatov, S. and Zhumaniyozov, S., 2022, October. Computer simulation of two-dimensional nonstationary problems of heat conduction for composite materials using the FEM. In AIP Conference Proceedings (Vol. 2637, No. 1). AIP Publishing.
34. Xu, D., Xiong, S., Meng, F., Wang, B. and Li, R., 2022. An analytic model of transient heat conduction for bi-layered flexible electronic heaters by symplectic superposition. Micromachines, 13(10), p.1627.
35. Moon, S.H., Lee, D., Kim, M. and Kim, Y., 2022. Evaporation heat transfer coefficient and frictional pressure drop of R600a in a micro-fin tube at low mass fluxes and temperatures. International Journal of Heat and Mass Transfer, 190, p.122769.
36. Li, H. and Hrnjak, P., 2022. Heat transfer coefficient, pressure gradient, and flow patterns of R1233zd (E) and R1336mzz (Z) evaporating in a microchannel tube. International Journal of Heat and Mass Transfer, 182, p.121992.
37. Sutthivirode, K. and Thongtip, T., 2022. Experimental investigation of a two-phase ejector installed into the refrigeration system for performance enhancement. Energy Reports, 8, pp.7263-7273.
38. Sutthivirode, K. and Thongtip, T., 2021. Feasibility study and in-depth performance assessment of needle valve using as expansion device in refrigeration system. Case Studies in Thermal Engineering, 25, p.100923.
39. Singmai, Wichean, Kasemsil Onthong, and Tongchana Thongtip. 2023. "Experimental Investigation of the Improvement Potential of a Heat Pump Equipped with a Two-Phase Ejector" Energies 16, no. 16: 5889. https://doi.org/10.3390/en16165889